

Constraints on exotic spin-dependent interactions between electrons from helium fine-structure spectroscopy

Filip Ficek^{1,*}, Derek F. Jackson Kimball², Mikhail Kozlov^{3,4},
Nathan Leefer⁵, Szymon Pustelny¹, and Dmitry Budker^{5,6,7}

¹ *Institute of Physics, Jagiellonian University, Lojasiewicza 11, 30-348 Kraków, Poland*

² *Department of Physics, California State University - East Bay, Hayward, California 94542-3084, USA*

³ *Petersburg Nuclear Physics Institute, Gatchina 188300, Russia*

⁴ *St. Petersburg Electrotechnical University LETI, Prof. Popov Str. 5, 197376 St. Petersburg*

⁵ *Helmholtz Institute Mainz, Johannes Gutenberg University, 55099 Mainz, Germany*

⁶ *Department of Physics, University of California at Berkeley, Berkeley, California 94720-7300, USA*

⁷ *Nuclear Science Division, Lawrence Berkeley National Laboratory, Berkeley, California 94720, USA*

(Dated: June 14, 2022)

Agreement between theoretical calculations of atomic structure and spectroscopic measurements is used to constrain possible contribution of exotic spin-dependent interactions between electrons to the energy differences between states in helium-4. In particular, constraints on dipole-dipole interactions associated with the exchange of pseudoscalar bosons (such as axions or axion-like particles, ALPs) with masses 10^{-2} eV $\lesssim m \lesssim 10^4$ eV are improved by a factor of ~ 100 . The first atomic-scale constraints on several exotic velocity-dependent dipole-dipole interactions are established as well.

PACS numbers: 31.15.aj, 31.30.-i, 12.60.-i

Heretofore undiscovered spin-dependent interactions [1, 2] naturally arise in theories predicting new bosons such as axions [3–7], familons [8, 9], majorons [10, 11], arions [12], new spin-0 or spin-1 gravitons [13–16], Kaluza-Klein zero modes in string theory [17], paraphotons [18], and new Z' bosons [19]. Such new bosons are connected to possible explanations of the nature of dark matter [20], dark energy [21, 22], the strong-CP problem [1], and the hierarchy problem [23].

The most commonly employed framework for the purpose of comparing different experimental searches for exotic spin-dependent interactions is that introduced in Ref. [1] to describe long-range spin-dependent potentials associated with the axion and extended in Ref. [2] to encompass long-range potentials associated with any generic spin-0 or spin-1 boson. The spin-dependent potentials enumerated in Ref. [2] are characterized by dimensionless coupling constants that specify the strength of the interaction between various particles and a characteristic range λ for the interaction associated with the reduced Compton wavelength of the new boson of mass m_0 , $\lambda = \hbar/(m_0c)$ where \hbar is the reduced Planck constant and c is the speed of light. Depending on the nature of the new interaction, different particles will have different coupling constants. In the present work we study dipole-dipole interactions between electrons at the atomic scale through investigation of the electronic structure of helium-4. The most stringent constraints on exotic dipole-dipole interactions between electrons have been established by torsion-pendulum experiments [24–26] at the laboratory scale ($\lambda \gtrsim 1$ cm) and by measurements on trapped ions [27] at the micron scale ($10 \mu\text{m} \lesssim$

$\lambda \lesssim 1$ m). The only existing constraints on exotic dipole-dipole interactions between electrons at the atomic scale come from positronium spectroscopy [27, 28, 43], which carries a caveat that CPT invariance must be implicitly assumed in order to translate the constraint to electrons [27].

Spectroscopic measurements of helium have been a popular research topic for several decades [30–34]. These investigations enable determination of energy-level structure of the element with a good precision. In particular, Feng *et al.* recently [30] determined the frequency of the $2^3P_1 \rightarrow 2^3P_2$ transition with an uncertainty of 0.36 kHz (1- σ level) while, measurements of the $2^3S_1 \rightarrow 2^3P_{0,1,2}$ transitions, performed by Pastor *et al.*, measured the frequency with uncertainty of ~ 2 kHz [31].

Worse precision has so far been obtained for theoretical calculations of the helium energy structure. To date, the most precise theoretical calculations have been performed by Pachucki and Yerokhin [35, 36], who used perturbation theory to calculate the helium fine-structure splittings in a perturbation theory up to the $m_e\alpha^7$ order (in relativistic units), where m_e is the electron mass and α is the fine-structure constant. This enabled calculations of $2^3P_{0,1,2}$ level splittings with uncertainty of ~ 2 kHz [35]. At the same time, the energy differences between the 2^3S_1 and $2^3P_{0,1,2}$ levels were calculated to the $m_e\alpha^6$ order, enabling determination of the transition frequencies with uncertainties of ~ 3.0 MHz [36].

In the context of comparison of experimental results and theoretical calculations, it is noteworthy that in quantum systems, e.g., atoms, a subtle systematic effect, arising from quantum interference of a given transition with off-resonance excitations, can affect positions of measured spectral lines [37–40]. As reported in Ref. [40], this effect causes the shift of the helium $2^3P_1 \rightarrow 2^3P_2$ transition frequency by 10 kHz. Since this is larger than

*Electronic address: filip.ficek@student.uj.edu.pl

the uncertainty of experimental data and theoretical calculations, in our considerations of helium fine structure, we use the value of the transition frequency reported in Ref. [30], where this effect was taken into account. On the other hand, the theoretical uncertainties of the $2^3S_1 \rightarrow 2^3P_{0,1,2}$ transition frequencies are so large that the interference effect can be neglected.

In this work, we determine limits on the coupling constants for various exotic interactions between electron spins from their possible effect on transition energies. By comparing the experimental and theoretical results, we extract a maximal possible energy contribution ΔE that may come from exotic interactions at the 90% confidence level (see Appendix A for details of how ΔE is determined).

Table I presents the contemporary theoretical and ex-

perimental energy values for various ^4He transitions used in our calculations of limits on exotic spin-dependent interactions.

In Ref. [2], Dobrescu and Mocioiu introduced 16 independent scalar spin-spin interactions. They were constructed as a linearly independent, rotationally-invariant scalars (details are explained in Appendix B). For studies of exotic spin couplings using ^4He , only those potentials invariant under permutation of identical fermions, spatial inversion, and time reversal are relevant. These three conditions ensure a non-zero result of calculations of exotic-field-induced shifts of energy levels in first-order perturbation theory. There are four potentials that satisfy these requirements. In the position representation they have the form

$$V_2 = \frac{g_2^e g_2^e}{4\pi\hbar c} \hbar c (\mathbf{s}_1 \cdot \mathbf{s}_2) \frac{e^{-r_{12}/\lambda}}{r_{12}}, \quad (1)$$

$$V_3 = \frac{g_3^e g_3^e}{4\pi\hbar c} \frac{\hbar^3}{4m_e^2 c} \left[\mathbf{s}_1 \cdot \mathbf{s}_2 \left(\frac{1}{\lambda r_{12}^2} + \frac{1}{r_{12}^3} \right) - (\mathbf{s}_1 \cdot \mathbf{e}_{12}) (\mathbf{s}_2 \cdot \mathbf{e}_{12}) \left(\frac{1}{\lambda^2 r_{12}} + \frac{3}{\lambda r_{12}^2} + \frac{3}{r_{12}^3} \right) \right] e^{-r_{12}/\lambda}, \quad (2)$$

$$V_4 = \frac{g_4^e g_4^e}{4\pi\hbar c} \frac{i\hbar^3}{4m_e^2 c} (\mathbf{s}_1 + \mathbf{s}_2) \cdot \left[(\nabla_1 - \nabla_2) \times \mathbf{r}_{12}, \left(\frac{1}{r_{12}^3} + \frac{1}{\lambda r_{12}^2} \right) e^{-r_{12}/\lambda} \right]_+, \quad (3)$$

$$V_8 = \frac{g_8^e g_8^e}{4\pi\hbar c} \frac{\hbar^3}{4m_e^2 c} \left[\mathbf{s}_1 \cdot (\nabla_1 - \nabla_2), \left[\mathbf{s}_2 \cdot (\nabla_1 - \nabla_2), \frac{e^{-r_{12}/\lambda}}{r_{12}} \right]_+ \right]_+, \quad (4)$$

where $g_i^e g_i^e / (4\pi\hbar c)$ is the dimensionless coupling constant of the i -th interaction between the electrons (this is the notation of Refs. [1, 2, 27, 41], where g^e refers to the coupling of an electron to the exotic boson), r_{12} is the distance between the electrons, $\mathbf{e}_{12} = \mathbf{r}_{12}/r_{12}$ is the unit vector in the direction from the first electron to the second electron, ∇_1 and ∇_2 are vector differential operators in position space for the first and second particle respectively, and $\mathbf{s}_1, \mathbf{s}_2$ are spins of the interacting electrons. By $[\cdot, \cdot]_+$ we denote an anticommutator.

These potentials are results of the exchange of exotic bosons [2, 42, 43]: scalar (V_4), pseudoscalar (V_3), vector (V_3), and axial-vector (V_2, V_3, V_8).

Note that the velocity-dependent potentials (3, 4) have here different forms than in Ref. [2] and other papers considering non-static exotic interactions [44]. This difference comes from the fact, that the velocity-dependent potentials in Refs. [2, 44] are in fact presented in a „mixed” representation (not a position representation, as stated). We discuss this further in the Appendix B.

The strength of any hypothetical exotic spin-dependent interactions between two electrons is orders of magnitude smaller than their electromagnetic interaction. Based on this fact, high precision is not required in calculation of the perturbation due to the exotic effects

and it is enough to calculate the exotic contributions to first order in perturbation theory. For these calculations, approximate wave functions of electrons in helium may be assumed. Here, we use the electron wave functions of the $n = 2$ state of orthohelium ($S = 1$), obtained with the variational method (see, for example, Ref. [45]). In Table II one can find the ionization energies calculated with these wave functions ε_{th} compared with the experimental values ε_{exp} . The difference between them is just several percent which suggests that these functions can be safely used in our calculations.

The spatial electron wave function for the He 2^3S_0 state is given by [45]

$$\psi^S = C^S \left[e^{-Z_i^S r_1 - Z_a^S r_2/2} \left(\frac{Z_a^S r_2}{2} - 1 \right) - e^{-Z_i^S r_2 - Z_a^S r_1/2} \left(\frac{Z_a^S r_1}{2} - 1 \right) \right], \quad (5)$$

where the Z_a^S, Z_i^S, C^S values are given in Table II and r_1, r_2 are in Bohr radii. The spatial electron wave function is antisymmetric with respect to the $1 \leftrightarrow 2$ electron exchange, so the spin wave function must be symmetric (as we may expect for orthohelium) and the total spin is $S = 1$. Since the 2^3S_0 state is only used to constrain

TABLE I: Comparison of theoretical (QED-based) and experimental transition energies values between various helium states.

	Theoretical		Experimental		Difference	ΔE
$2^3P_1 - 2^3P_2$	2 291 178.9(1.7) kHz	[35]	2 291 177.69(36) kHz	[30]	1.2(1.7) kHz	4.6 kHz
$2^3P_0 - 2^3P_2$	31 908 131.2(1.8) kHz	[35]	31 908 131.25(30) kHz	[32]	0.1(1.8) kHz	3.2 kHz
$2^3P_0 - 2^3P_1$	29 616 952.3(1.7) kHz	[35]	29 616 951.66(70) kHz	[33]	0.6(1.8) kHz	3.7 kHz
$2^3P_0 - 2^3S_1$	276 764 094.7(3.0) MHz	[36]	276 764 094.7073(21) MHz	[31]	0.0(3.0) MHz	
$2^3P_1 - 2^3S_1$	276 734 477.7(3.0) MHz	[36]	276 734 477.7525(20) MHz	[31]	0.1(3.0) MHz	
$2^3P_2 - 2^3S_1$	276 732 186.1(2.9) MHz	[36]	276 732 186.621(15) MHz	[31]	0.5(2.9) MHz	

TABLE II: Values of constants in the wave functions and ionization energies (in Rydbergs).

	Z_i	Z_a	C	ε_{th}	ε_{exp}
2^3S	2.01	1.53	0.43247	0.334	0.350
2^3P	1.99	1.09	0.097969	0.262	0.266

the V_2 potential, where the electron spins appear in the formula via the $\mathbf{s}_1 \cdot \mathbf{s}_2$ term, we do not have to consider explicitly the spin part of the wave function as for ortho-helium

$$\mathbf{s}_1 \cdot \mathbf{s}_2 |\psi^S\rangle = \frac{1}{2}(\mathbf{S}^2 - \mathbf{s}_1^2 - \mathbf{s}_2^2) |\psi^S\rangle = \frac{1}{4} |\psi^S\rangle. \quad (6)$$

The spatial components of the 2^3P -state wave functions are approximated by [45]

$$\begin{aligned} \Psi_1^P &= -C^P (F(r_1, r_2) \sin \theta_1 e^{i\phi_1} - F(r_2, r_1) \sin \theta_2 e^{i\phi_2}), \\ \Psi_0^P &= \sqrt{2} C^P (F(r_1, r_2) \cos \theta_1 - F(r_2, r_1) \cos \theta_2), \\ \Psi_{-1}^P &= C^P (F(r_1, r_2) \sin \theta_1 e^{-i\phi_1} - F(r_2, r_1) \sin \theta_2 e^{-i\phi_2}), \end{aligned} \quad (7)$$

where

$$F(r_1, r_2) = r_1 e^{-Z_a^P r_1/2 - Z_i^P r_2}, \quad (8)$$

where the Z_a^P, Z_i^P, C^P values are given in Table II. We associate these antisymmetric wave functions with symmetric spin functions using the Clebsch-Gordan coefficients coming from addition of angular momenta $L = 1$ and $S = 1$. In the following sections we will be performing calculations using wave functions $|\psi_{J,m_J}^P\rangle$

$$|\Psi_{2,2}^P\rangle = \Psi_1^P |\uparrow\uparrow\rangle, \quad (9)$$

$$|\Psi_{2,1}^P\rangle = \sqrt{\frac{1}{2}} \Psi_0^P |\uparrow\uparrow\rangle + \frac{1}{2} \Psi_1^P (|\uparrow\downarrow\rangle + |\downarrow\uparrow\rangle), \quad (10)$$

where $|\uparrow\downarrow\rangle = |m_{s_1} = 1/2; m_{s_2} = -1/2\rangle$ and $m_{s_{1,2}}$ are the magnetic quantum numbers of the 1st and 2nd electron, respectively.

For every considered potential V_i we can estimate an associated energy shift between states $|\psi_a\rangle$ and $|\psi_b\rangle$ using first-order perturbation theory and the approximate wave functions listed above:

$$\Delta U_{ab,i}(m_0) = \langle \psi_a | \mathcal{V}_i(m_0) | \psi_a \rangle - \langle \psi_b | \mathcal{V}_i(m_0) | \psi_b \rangle, \quad (11)$$

where $\mathcal{V}_i(m_0)$ is a potential V_i divided by the dimensionless constant $g_i^e g_i^e / (4\pi\hbar c)$. Values for $\Delta U_{ab,i}$ were calculated by numerical integration for several m_0 values and then an interpolation was performed in order to obtain a continuous function $\Delta U_{ab,i}(m_0)$. For potentials V_3, V_4 , and V_8 curves describing the constraints on $g_i^e g_i^e / (4\pi\hbar c)$ were obtained for different values of m_0 by substituting the appropriate ΔE (the one connected with $2^3P_1 - 2^3P_2$ transition) from Table I into the relation:

$$\frac{g_i^e g_i^e}{4\pi\hbar c}(m_0) \leq \frac{\Delta E}{\Delta U_{ab,i}(m_0)}. \quad (12)$$

For $m_0 \gtrsim 3000$ eV the Compton wavelength of the mediating boson is shorter than the average interparticle separation between electrons in the helium atom. Because of that, the transition frequency becomes insensitive to the considered potentials for $m_0 \gtrsim 3000$ eV as seen in the parameter exclusion plots.

The results for the V_3 potential are presented in Fig. 1. The other results in this Figure come from Ref. [27]. It can be seen that comparison between theory and experiment for helium fine structure yields the best constraints in the considered mass range (two orders of magnitude more stringent than the previous ones).

In order to calculate constraints for the V_4 potential we use its reduced form. As shown in Appendix B, the potential (3) can be written as $V_4 = \mathbf{S} \cdot [\mathbf{p}_{12} \times \mathbf{r}_{12}, f(r)]_+$, where \mathbf{r} and \mathbf{p} denote respectively the differences between position and momentum operators for the electrons, and $f(r)$ is the spatial part of the potential with appropriate constants. One can write $\mathbf{p}_{12} = -i\hbar\nabla_{r_{12}}$, and then $\nabla_{r_{12}} f(r_{12}) = \mathbf{e}_{12} \partial_{r_{12}} f(r_{12})$. We see that when gradient in the commutator operates on $f(r)$ we get $-i(\mathbf{e}_{12} \times \mathbf{e}_{12}) \partial_{r_{12}} f(r_{12}) = 0$. We conclude, that V_4 may be written as

$$V_4 = \mathbf{S} \cdot [\mathbf{p}_{12} \times \mathbf{r}_{12}, f(r_{12})]_+ = 2f(r_{12})\mathbf{S} \cdot (\mathbf{p}_{12} \times \mathbf{r}_{12}) = -2f(r_{12})\mathbf{S} \cdot (\mathbf{r}_{12} \times \mathbf{p}_{12}), \quad (13)$$

where we have used the fact that $(\mathbf{p}_{12} \times \mathbf{r}_{12})_i = \epsilon_{ijk} p_{12}^j r_{12}^k = \epsilon_{ijk} r_{12}^k p_{12}^j = -(\mathbf{r}_{12} \times \mathbf{p}_{12})_i$. The expectation value of this operator, needed for Eq. (11), can be obtained using reduced matrix elements. For state $|JM11\rangle = |JM11\rangle$ we have

$$\langle JM11|V_4|JM11\rangle = - \left\{ \begin{matrix} J & 1 & 1 \\ 1 & 1 & 1 \end{matrix} \right\} \langle S||\mathbf{S}||S\rangle_{S=1} \langle L||f(r_{12})\mathbf{r}_{12} \times \mathbf{p}_{12}||L\rangle_{L=1} = \frac{J(J+1)-4}{2\sqrt{6}} \langle 1||f(r_{12})\mathbf{r}_{12} \times \mathbf{p}_{12}||1\rangle, \quad (14)$$

where we have introduced the 6j symbols [46, 47] and used the fact that $\langle S||\mathbf{S}||S\rangle = \sqrt{S(S+1)(2S+1)}$. Calculating the remaining reduced matrix element yields:

$$\langle JM11|V_4|JM11\rangle = \frac{1}{2}(J(J+1)-4)\langle L|\tilde{f}(r_{12})(1-D_{12}-D_{21})|L\rangle_{L=1}, \quad (15)$$

where

$$D_{jk} = ir_j \sin\theta_j \left[\sin(\phi_j - \phi_k) \left(\sin\theta_k \frac{\partial}{\partial r_k} + \frac{\cos\theta_k}{r_k} \frac{\partial}{\partial \theta_k} \right) - \cos(\phi_j - \phi_k) \frac{1}{r_k \sin\theta_k} \frac{\partial}{\partial \phi_k} \right] \quad (16)$$

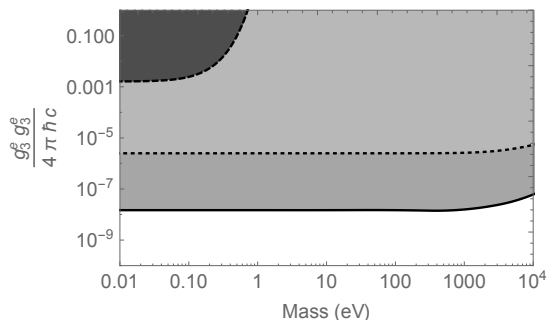


FIG. 1: Constraints (at the 90% confidence level) on the dimensionless coupling constant $g_3^e g_3^e / (4\pi\hbar c)$ as a function of the boson mass. The dotted line and dark gray fill shows the constraint for electrons from Ref. [27]. The dashed line and light gray fill show the constraint derived from analysis of positronium, also discussed in [27]. The solid line and medium gray fill shows the constraint from a comparison between theory and experiment for the $2^3P_2 \leftrightarrow 2^3P_1$ transition frequency in He.

and $|L=1\rangle$ is a state represented by the first wave function in Eq. (7).

We use this reduced form of V_4 to numerically obtain $\Delta U_{ab,i}(m_0)$ function and finally get $g_i^e g_i^e / 4\pi\hbar c(m_0)$ sketched in Fig. 2.

The results for the V_8 potential are presented in Fig. 3. Constraints for V_8 electron coupling constant were obtained earlier using geoelectron experiments [44], which considered boson masses less than 10^{-10} eV, yielding constraints $g_8^e g_8^e / (4\pi\hbar c) \lesssim 10^{-36}$ in the massless limit.

The analysis for the V_2 potential differs somewhat from that carried out for the other potentials. Spin operators

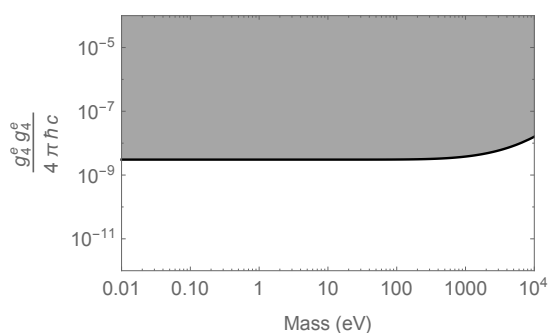


FIG. 2: Constraints (at the 90% confidence level) on the dimensionless coupling constant $g_4^e g_4^e / (4\pi\hbar c)$ as a function of the boson mass coming from a comparison between theory and experiment for the $2^3P_2 \leftrightarrow 2^3P_1$ transition frequency in He.

in the V_2 potential are of the form $\mathbf{s}_1 \cdot \mathbf{s}_2$ so for orthoheium wave functions $|\psi\rangle$ we have $\mathbf{s}_1 \cdot \mathbf{s}_2 |\psi\rangle = \frac{1}{4} |\psi\rangle$. This means that the analysis for this case is based on evaluation of the $\langle \psi | \exp(-r_{12}/\lambda) / r_{12} | \psi \rangle$ matrix elements.

The V_2 potential does not split energy levels of different J and the same L and S , but only shifts each such level by the same amount. This means that in order for such an energy shift to be experimentally observable we need another reference state outside the fine-structure manifold. For this purpose, based on the available experimental data and theoretical calculations, a natural choice is a comparison between the 2^3S_1 and 2^3P states. The fact that the V_2 potential does not remove J degeneracy implies that the $2^3S_1 - 2^3P_J$ comparison does not depend on the particular choice of $|J, m_J\rangle$. Therefore we use all the values of differences between experimental and theo-

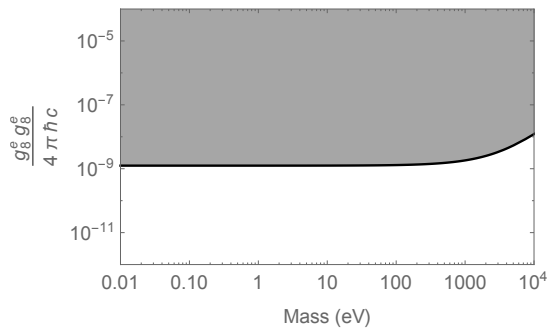


FIG. 3: Constraints (at the 90% confidence level) on the dimensionless coupling constant $g_8^e g_8^e / (4\pi\hbar c)$ as a function of the boson mass coming from a comparison between theory and experiment for the $2^3P_2 \leftrightarrow 2^3P_1$ transition frequency in He.

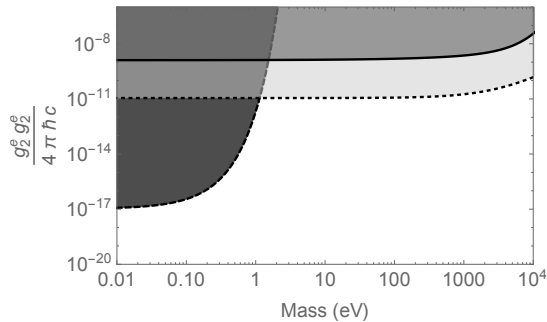


FIG. 4: Constraints (at the 90% confidence level) on the dimensionless coupling constant $g_2^e g_2^e / (4\pi\hbar c)$ as a function of the boson mass. The dotted line and dark gray fill shows the constraint for electrons from Ref. [27]. The dashed line and light gray fill show the constraint derived from analysis of positronium, also discussed in [27]. The solid line and medium gray fill shows the constraint from a comparison between theory and experiment for the $2^3S_1 \leftrightarrow 2^3P$ transition frequency in He.

retical transition energies between states $2^3S - 2^3P$ from Table I. Treating these differences as ΔE from formula (12) we get a function $g_i^e g_i^e / (4\pi\hbar c)(m_0)$ for every transition, along with the uncertainty. We calculate weighted mean of these with its uncertainty, and take a sum of this mean and a doubled uncertainty as the limit. The results are presented in Fig. 4. The obtained constraints are worse than the ones obtained using positronium atom [27], but we note that positronium constrains the interaction between positrons and electrons which can only be directly compared with the electron-electron interaction under the assumption of CPT invariance.

In conclusion, by comparing the results of precision spectroscopic measurements in ^4He with theoretical calculations of the corresponding energy intervals, we establish constraints on possible exotic interactions that could arise due to the exchange of bosonic fields, as introduced in the theoretical framework of Refs. [1, 2]. We pointed out an inconsistency of the operator definitions in Ref.

[2] and perform the analysis with the corrected operators. We improve constraints on the strength of some of the exotic interactions by two orders of magnitude and constrain others for the first time.

We expect He spectroscopy to become an even more sensitive probe of exotic electron-electron interactions as atomic theory and experiment become more precise.

Acknowledgments

The authors acknowledge Victor Flambaum, Krzysztof Pachucki and Savely G. Karshenboim for fruitful discussions and useful remarks. This project was partially supported by the European Research Council (ERC) under the European Unions Horizon 2020 research and innovation programme (grant agreement No 695405), Russian Foundation for Basic Research Grant No. 14-02-00241, the Polish Ministry of Science and Higher Education within the Iuventus Plus program (grant 0390/IP3/2015/73), National Science Foundation under grant PHY-1307507, the Heising-Simons and Simons Foundations, and a Marie Curie International Incoming Fellowship within the 7th European Community Framework Programme. MK is grateful to Mainz Institute for Theoretical Physics (MITP) for its hospitality and support.

Appendix A: Analysis of the experimental and theoretical data

For fine-structure transitions, where we use only one value, our method is as follows: we define $\Delta E = \max\{|\mu + L|, |\mu - L|\}$, where μ is the mean difference between theoretical and experimental transition energies and L is determined in such a way that

$$0.9 = \int_{-L}^{+L} \frac{1}{\sqrt{2\pi}\sigma} e^{-(x-\mu)^2/(2\sigma^2)} dx, \quad (\text{A1})$$

where σ is the resultant uncertainty, originating from theoretical (σ_{th}) and experimental (σ_{exp}) uncertainties combined in quadrature, $\sigma^2 = \sigma_{th}^2 + \sigma_{exp}^2$. This method was used for the potentials V_3, V_4 , and V_8 .

Apart from these calculations, we have also performed for these potentials an analysis similar to the one performed for potential V_2 – we have used differences between theoretical and experimental transition values for all three transitions to calculate weighted mean of $g_2^e g_2^e / (4\pi\hbar c)$. Constraints obtained this way are twice more stringent as the ones plotted on Figs. 1-3. In spite of this fact we do not use them, as they include a systematic error due to the shifts from a distant neighboring resonance described in the paper.

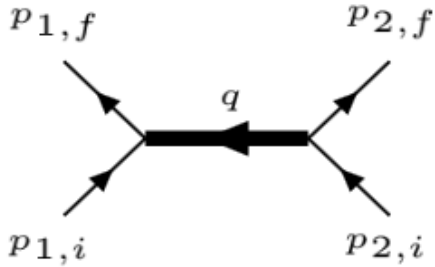


FIG. 5: Graph of an interaction between two electrons mediated by a light boson.

Appendix B: Potentials in position representation

Here we will show the way Eqs. (1-4) were derived and explain why they differ from their counterparts from [2].

Let us consider an interaction between two electrons mediated by a light boson. A corresponding Feynman diagram is shown in Fig. 5, where $\mathbf{p}_{1,i}$ and $\mathbf{p}_{1,f}$ are initial and final momenta of the first electron ($\mathbf{p}_{2,i}$ and $\mathbf{p}_{2,f}$ are analogously initial and final momentum of the second electron), and \mathbf{q} is the momentum of the light interacting boson. We may describe this interaction in the center of mass frame using just two vectors

$$\mathbf{P} = \frac{1}{2}(\mathbf{p}_{1,f} + \mathbf{p}_{1,i}), \quad (\text{B1})$$

$$\mathbf{q} = \mathbf{p}_{1,f} - \mathbf{p}_{1,i}. \quad (\text{B2})$$

In their paper [2] Dobrescu and Mocioiu construct 16 independent, rotationally invariant scalars consisting of the vectors $\mathbf{P}, \mathbf{q}, \mathbf{s}_1, \mathbf{s}_2$, where $\mathbf{s}_1, \mathbf{s}_2$ are the spin of the first and second electron, respectively. These scalars are operators in momentum representation (momentum operators are multiplication operators). Due to the focus of this paper, we will consider four of them that are spin-dependent, symmetric with respect to a permutation of identical fermions, and invariant under spatial inversion and time reversal. In natural units ($c = \hbar = 1$) they have the form

$$\mathcal{O}_2 = \mathbf{s}_1 \cdot \mathbf{s}_2, \quad (\text{B3})$$

$$\mathcal{O}_3 = \frac{1}{m_e^2}(\mathbf{s}_1 \cdot \mathbf{q})(\mathbf{s}_2 \cdot \mathbf{q}), \quad (\text{B4})$$

$$\mathcal{O}_4 = \frac{i}{2m_e^2}(\mathbf{s}_1 + \mathbf{s}_2) \cdot (\mathbf{P} \times \mathbf{q}), \quad (\text{B5})$$

$$\mathcal{O}_8 = \frac{1}{m_e^2}(\mathbf{s}_1 \cdot \mathbf{P})(\mathbf{s}_2 \cdot \mathbf{P}), \quad (\text{B6})$$

where m_e is an electron mass. Note that it is $i\mathbf{q}$, rather than \mathbf{q} - that is a Hermitian operator, and is why the \mathcal{O}_4 operator in Eq.(B5), which is linear in \mathbf{q} , is imaginary.

In Sec. 3 of Ref. [2] these operators are converted into potentials by making a Fourier transform from \mathbf{q}

to $\mathbf{r}_{12} = \mathbf{r}_1 - \mathbf{r}_2$ (we introduce here a slightly different notation than the original one). Note that this is a mixed representation as the authors still keep $\mathbf{v} = \mathbf{P}/m_e$ as a variable, rather than an operator (see Eq. (3.2) in Ref. [2]). In the coordinate (or position) representation all expressions which include \mathbf{v} should be written in terms of an operator $\hat{\mathbf{v}}$, which is related to the gradient.

Let us consider a potential of the form $\mathbf{P}V(r_{12})$:

$$\begin{aligned} & \langle \psi_f(r_1, r_2) | \mathbf{P}V(r_{12}) | \psi_i(r_1, r_2) \rangle \\ &= \frac{1}{2} \langle \psi_f(r_1, r_2) | \mathbf{p}_{1,f} V(r_{12}) + V(r_{12}) \mathbf{p}_{1,i} | \psi_i(r_1, r_2) \rangle \\ &= \frac{1}{2} \langle \psi_f(r_1, r_2) | \hat{\mathbf{p}}_1 V(r_{12}) + V(r_{12}) \hat{\mathbf{p}}_1 | \psi_i(r_1, r_2) \rangle \\ &= \frac{1}{2} \langle \psi_f(r_1, r_2) | [\hat{\mathbf{p}}_1, V(r_{12})]_+ | \psi_i(r_1, r_2) \rangle, \quad (\text{B7}) \end{aligned}$$

where $|\psi_i(r_1, r_2)\rangle$ and $|\psi_f(r_1, r_2)\rangle$ are the initial and final states of the considered system, respectively, and $\hat{\mathbf{p}}_1$ is the momentum operator of the first electron. This step introducing the anticommutator was omitted in Ref. [2] resulting in mixed representation of non-static potentials, where \mathbf{v} is a variable rather than an operator.

Having this in mind, we perform the Fourier transform in order to go from the momentum representation to the position representation:

$$\mathcal{V}_i(\mathbf{r}_{12}, \mathbf{p}_{12}) = - \int \frac{d^3q}{(2\pi)^3} e^{i\mathbf{q}\mathbf{r}_{12}} \mathcal{P}(\mathbf{q}^2) \mathcal{O}_i(\mathbf{q}, \mathbf{P}), \quad (\text{B8})$$

where $\mathcal{P}(\mathbf{q}^2)$ is a propagator. We are interested in Lorentz invariant exotic interactions communicated by a single boson with mass m_0 , which implies a propagator of the form [2, 48]

$$\mathcal{P}(\mathbf{q}^2) = - \frac{1}{\mathbf{q}^2 + m_0^2}, \quad (\text{B9})$$

where m_0 is the intermediate boson mass. Useful formulae for these Fourier transforms may be found in Appendix B of Ref. [2].

As an example we will derive the position-representation form of the V_4 potential (3). We begin with the momentum-representation form in natural units, Eq. (B5). By performing Fourier transform we obtain

$$\begin{aligned} \tilde{V}_4 &= \int \frac{d^3q}{(2\pi)^3} e^{i\mathbf{q}\mathbf{r}_{12}} \frac{\mathcal{O}_4}{\mathbf{q}^2 + m_0^2} \quad (\text{B10}) \\ &= \frac{i}{2m_e^2} (\mathbf{s}_1 + \mathbf{s}_2) \cdot \left(\mathbf{P} \times \int \frac{d^3q}{(2\pi)^3} e^{i\mathbf{q}\mathbf{r}_{12}} \frac{\mathbf{q}}{\mathbf{q}^2 + m_0^2} \right) \\ &= - \frac{1}{8\pi m_e^2} (\mathbf{s}_1 + \mathbf{s}_2) \cdot \left(\mathbf{P} \times \frac{\mathbf{r}_{12}}{r_{12}^3} \right) (1 + m_0 r_{12}) e^{-m_0 r_{12}}. \end{aligned}$$

Now let us apply similar reasoning as in case of Eq. (B7), but for the operator $\mathbf{P} \times \mathbf{r}_{12} V(r_{12})$. The j -th component of this operator matrix element will be (using the Einstein summation convention):

$$\begin{aligned}
& \langle (\psi_f(r_1, r_2) | \mathbf{P} \times \mathbf{r}_{12} V(r_{12}) | \psi_i(r_1, r_2)) \rangle_j = \left(\frac{1}{2} \langle \psi_f(r_1, r_2) | (\mathbf{P}_{1,f} + \mathbf{P}_{1,i}) \times (\mathbf{r}_{12} V(r_{12})) | \psi_i(r_1, r_2) \rangle \right)_j \\
& = \frac{1}{2} \varepsilon_{jkl} \langle \psi_f(r_1, r_2) | (p_{1,f}^k + p_{1,i}^k) r_{12}^l V(r_{12}) | \psi_i(r_1, r_2) \rangle = \frac{1}{2} \varepsilon_{jkl} \langle \psi_f(r_1, r_2) | (p_{1,f}^k r_{12}^l V(r_{12}) + V(r_{12}) r_{12}^l p_{1,i}^k) | \psi_i(r_1, r_2) \rangle \\
& = \frac{1}{2} \varepsilon_{jkl} \langle \psi_f(r_1, r_2) | (p_{1,f}^k r_{12}^l V(r_{12}) + V(r_{12}) p_{1,i}^k r_{12}^l) | \psi_i(r_1, r_2) \rangle = \frac{1}{2} \varepsilon_{jkl} \langle \psi_f(r_1, r_2) | [p_{1,f}^k r_{12}^l, V(r_{12})]_+ | \psi_i(r_1, r_2) \rangle \\
& = \frac{1}{2} \langle \psi_f(r_1, r_2) | [(\mathbf{P}_1 \times \mathbf{r}_{12})_j, V(r_{12})]_+ | \psi_i(r_1, r_2) \rangle,
\end{aligned}$$

where we have used the fact that $\varepsilon_{jkl} r^k p^l = \varepsilon_{jkl} p^l r^k + i\varepsilon_{jkl} \delta^{kl} = \varepsilon_{jkl} p^l r^k$. These calculations were performed in the center of mass frame of the two particles. In atomic physics we use the center of mass frame of an atom. We can convert our equations to it by substituting $\mathbf{p}_1 \rightarrow \mathbf{p}_1 - \frac{1}{2}(\mathbf{p}_1 + \mathbf{p}_2) = \frac{1}{2}(\mathbf{p}_1 - \mathbf{p}_2) = \frac{1}{2}\mathbf{p}_{12}$. When we put results of these calculations into Eq. (B10), we get

$$\tilde{V}_4 = -\frac{1}{16\pi m_e^2} (\mathbf{s}_1 + \mathbf{s}_2) \cdot \left[\mathbf{p}_{12} \times \mathbf{r}_{12}, \frac{1 + m_0 r_{12}}{r_{12}^3} e^{-m_0 r_{12}} \right]_+$$

This potential is what we used to calculate the contribution of the V_4 interaction to the He energy levels. The last

remaining steps are introducing the coupling constant, writing momenta as a differential operators, and inserting physical constants: c, \hbar, m_e , and the reduced Compton wavelength of the interaction boson $\lambda = \hbar/m_0 c$. These steps result in Eq. (3).

There is one remark to be noted. The framework introduced to deal with exotic potentials by Dobrescu and Mocioiu in [2] works only in the low-mass limit of the interacting boson. However, as we are interested in bosons with atomic-scale Compton wavelength, we can safely treat this framework as accurate.

-
- [1] J. E. Moody and F. Wilczek, Phys. Rev. D **30**, 130 (1984).
- [2] B. A. Dobrescu and I. Mocioiu, J. High Energy Phys. **11**, 5 (2006).
- [3] S. Weinberg, Phys. Rev. Lett. **40**, 223 (1978).
- [4] F. Wilczek, Phys. Rev. Lett. **40**, 279 (1978).
- [5] M. Dine, W. Fischler, and M. Srednicki, Phys. Lett. **104B**, 199 (1981).
- [6] M. Shifman, A. Vainshtein, , and V. Zakharov, Nucl. Phys. B **166**, 493 (1980).
- [7] J. Kim, Phys. Rev. Lett. **43**, 103 (1979).
- [8] F. Wilczek, Phys. Rev. Lett. **49**, 1549 (1982).
- [9] G. Gelmini, S. Nussinov, and T. Yanagida, Nucl. Phys. B **219**, 31 (1983).
- [10] G. Gelmini and M. Roncadelli, Phys. Lett. **99B**, 411 (1981).
- [11] Y. Chikashige, R. Mohapatra, and R. Peccei, Phys. Lett. **98B**, 265 (1981).
- [12] A. Ansel'm, Pis'ma Zh. Eksp. Teor. Fiz. **36**, 46 (1982).
- [13] J. Scherk, Phys. Lett. **88B**, 265 (1979).
- [14] D. E. Neville, Phys. Rev. D **21**, 2075 (1980).
- [15] D. E. Neville, Phys. Rev. D **25**, 573 (1982).
- [16] S. M. Carroll and G. B. Field, Phys. Rev. D **50**, 3867 (1994).
- [17] P. Svrcek and E. Witten, J. High Energy Phys. **06**, 051 (2006).
- [18] B. A. Dobrescu, Phys. Rev. Lett. **94**, 151802 (2005).
- [19] T. Appelquist, B. A. Dobrescu, and A. R. Hopper, Phys. Rev. D **68**, 035012 (2003).
- [20] G. Bertone, D. Hooper, and J. Silk, Phys. Rep. **405**, 279 (2005).
- [21] A. Friedland, H. Murayama, and M. Perelstein, Phys. Rev. D **67**, 043519 (2003).
- [22] V. Flambaum, S. Lambert, and M. Pospelov, Phys. Rev. D **80**, 105021 (2009).
- [23] P. W. Graham, D. E. Kaplan, S. Rajendran, Phys. Rev. Lett. **115**, 221801 (2015).
- [24] B. R. Heckel, W. A. Terrano, and E. G. Adelberger, Phys. Rev. Lett. **111**, 151802 (2013).
- [25] W. A. Terrano, E. G. Adelberger, J. G. Lee, and B. R. Heckel, Phys. Rev. Lett. **115**, 201801 (2015).
- [26] L. Hunter, J. Gordon, S. Peck, D. Ang, and J.-F. Lin, Science **339**, 928 (2013).
- [27] S. Kotler, R. Ozeri, and D. F. Jackson Kimball, Phys. Rev. Lett. **115**, 081801 (2015).
- [28] S. G. Karshenboim, Phys. Rev. Lett. **104**, 220406 (2010); Phys. Rev. D **82**, 073003 (2010); Phys. Rev. D **82**, 113013 (2010).
- [29] T. M. Leslie, E. Weisman, R. Khatiwada, and J. C. Long, Phys. Rev. D **89**, 114022 (2014).
- [30] G.-P. Feng, X. Zheng, Y. R. Sun, S.-M. Hu, Phys. Rev. A **91**, 030502 (2015).
- [31] P. Cancio Pastor, G. Giusfredi, P. De Natale, Phys. Rev. Lett. **92**, 023001 (2004).
- [32] M. Smiciklas, D. Shiner, Phys. Rev. Lett. **105**, 123001 (2010).
- [33] T. Zelevinsky, D. Farkas, G. Gabrielse, Phys. Rev. Lett. **95**, 203001 (2005).
- [34] P. Cancio, M. Artoni, G. Giusfredi, F. Minardi, F. S. Pavone, M. Inguscio, AIP Conf. Proc. **477**, 42 (1999).
- [35] K. Pachucki, V. A. Yerokhin, Phys. Rev. Lett. **104**, 070403 (2010).
- [36] V. A. Yerokhin, K. Pachucki, Phys. Rev. A **81**, 022507 (2010).
- [37] M. Horbatsch, E. A. Hessels, Phys. Rev. A **82**, 052519 (2010).
- [38] M. Horbatsch, E. A. Hessels, Phys. Rev. A **84**, 032508 (2011).

- [39] A. Marsman, M. Horbatsch, E. A. Hessels, Phys. Rev. A **86**, 040501 (2012)
- [40] A. Marsman, E. A. Hessels, M. Horbatsch, Phys. Rev. A **89**, 043403 (2014)
- [41] D. F. Jackson Kimball, A. Boyd, D. Budker, Phys. Rev. A **82**, 062714 (2010)
- [42] S. G. Karshenboim, V. V. Flambaum, Phys. Rev. A **84**, 064502 (2011)
- [43] T. M. Leslie, E. Weisman, R. Khatriwada, J. C. Long, Phys. Rev. D **89**, 114022 (2014)
- [44] L. R. Hunter, D. G. Ang, Phys. Rev. Lett. **112**, 091803 (2014)
- [45] H. A. Bethe, E. E. Salpeter, *Quantum Mechanics of One- and Two-Electron Atoms*, Academic Press Inc, New York, 1957
- [46] L.D. Landau, E. M. Lifshitz, *Quantum Mechanics: Non-Relativistic Theory*, Pergamon Press, 1977
- [47] D. A. Varshalovich, A. N. Moskalev, V. K. Khersonskii, *Quantum Theory of Angular Momentum*, World Scientific, 1988
- [48] V. B. Berestetskii, E. M. Lifshitz, L. P. Pitaevskii, *Quantum Electrodynamics*, Pergamon Press, 1982